

Passive tracers and active dynamics: A model study of hydrography and circulation in the northern North Atlantic

C. Mauritzen,¹ S. S. Hjøllo,² and A. B. Sandø³

Received 26 August 2005; revised 24 March 2006; accepted 28 April 2006; published 9 August 2006.

[1] A long-standing problem in oceanography has been to understand the relationship between what can be measured in the ocean, such as hydrography, and what cannot, such as the strength and structure of the complete Meridional Overturning Circulation (MOC) of the world oceans, commonly considered the main oceanic long-term modifier of Earth's climate. With the aid of a 50-year simulation from a numerical ice-ocean model we have investigated this relationship in the area of the northernmost extension of the MOC, in the subpolar and Nordic seas, on interannual timescales. We find that variability in the northward flux of salt and temperature in this region is controlled almost entirely by the volume flux, confirming that a knowledge of the variability of the circulation strength proper is necessary. The simulated hydrographic anomalies are within the range observed in the twentieth century; thus fundamental changes to the circulation were not expected nor found. It is seen that variability in either temperature or salinity does contain some information about the variability in current strength, because hydrography and circulation generally respond to the same atmospheric forcing in the North Atlantic sector. Whether it is temperature or salinity that contains the information is related to the parameter range of the equation of state at the location in question: If density depends primarily on temperature, then a salinity anomaly will tend to survive and vice versa. The oceanic response involves hydrographic changes and propagation of these, gyre strength changes, and changes in the MOC.

Citation: Mauritzen, C., S. S. Hjøllo, and A. B. Sandø (2006), Passive tracers and active dynamics: A model study of hydrography and circulation in the northern North Atlantic, *J. Geophys. Res.*, *111*, C08014, doi:10.1029/2005JC003252.

1. Introduction

[2] It was proposed roughly half a century ago that ocean circulation could fluctuate between states owing to the opposing effects temperature and salinity have on density [Stommel, 1961] and that it could even initiate an ice age [Ewing and Donn, 1956]. Oceanic circulation and hydrography (temperature and salinity, which through the equation of state yields density) are inherently linked through the basic balance of the equations of motion: the geostrophic balance, which links horizontal density gradients to vertical velocity gradients. (Hydrography is easier to observe than ocean currents, so the geostrophic balance has been used extensively for almost a century to infer ocean velocities. However, basic inadequacies of the relationship are problematic: one obtains the velocity shear only, not the absolute velocity. In addition, the geostrophic balance does not always hold.) They are also linked through buoyancy: Water sinks if it is denser than the water beneath. It is the latter connection that gives rise to the possibility of an ice age: Flushing of freshwater at the sea surface at northern

latitudes would prevent the surface waters from becoming dense enough to sink, no matter how cold they are, thus shutting down the Meridional Overturning Circulation (MOC) of the North Atlantic, and therefore, hypothetically, shutting down the northward oceanic transport of heat, leading, hypothetically, to a significantly colder climate.

[3] The last decades have indeed seen a significant change in the hydrography of the North Atlantic; the water masses have become less saline both in the Nordic seas and in the Subpolar Gyre [Lazier, 1995; Turrell *et al.*, 1999; Blindheim *et al.*, 2000; Dickson *et al.*, 2002; Curry *et al.*, 2003], and the potential for abrupt climatic change due to changes in ocean circulation has been studied extensively [see, e.g., Manabe and Stouffer, 1988, 1995; Marotzke and Willebrand, 1991]. Recently, the amount of freshwater added to the North Atlantic during the last 50 years has been quantified [Curry and Mauritzen, 2005], revealing a gradual buildup of freshwater in the Subpolar Gyre equaling an addition of some 19,000 km³ of freshwater, as well as certain periods when the buildup rate was much higher. These episodes have come to be known as "Great Salinity Anomalies" (GSAs). The largest of these, the GSA of the early 1970s, was first described by Dickson *et al.* [1988]. According to Curry and Mauritzen [2005], that GSA was associated with an accumulation of freshwater in the Subpolar Gyre of almost 0.1 Sv for a full 5-year period in the 1970s. Later GSAs occurred in the 1980s and the early

¹Climate Division, Norwegian Meteorological Institute, Oslo, Norway.

²Bjerknes Centre for Climate Research, Bergen, Norway.

³Nansen Environmental and Remote Sensing Center, Bergen, Norway.

1990s in the Subpolar Gyre [Belkin *et al.*, 1998], but these were smaller in magnitude according to the Curry and Mauritzen [2005] quantification.

[4] Although direct measurements of ocean circulation are sparse, it is quite evident that a major change or shutdown of ocean circulation has not occurred in the North Atlantic during the last 50 years (not even in the 1970s) despite the significantly changing hydrography. We investigate here the relationship between hydrography and circulation beneath threshold levels, i.e., when the changes are not large enough to result in fundamentally altered circulation pathways (a switch in “regime,” in Stommel’s vocabulary). We focus directly on the northward flow of warm waters toward northern Europe and the Nordic seas. At these high latitudes the MOC only partly represents the northward flow, because there is also a shallow return flow. Our goal is to gain further insight into the relationship between hydrography and the warm water currents toward the north, since we have measurements of the former for nearly a century, but much less information about the latter.

[5] We do the work with the aid of a numerical model, owing to the aforementioned sparse observational material. It is well known that numerical models in general struggle with simulating hydrography, so our results can be considered suggestive only. Nevertheless, we do know that this model has fared rather well in comparisons with observed hydrography [see, e.g., Nilsen *et al.*, 2003; Hátún *et al.*, 2005a, 2005b]. The findings are further evaluated against observations when possible. The paper is organized as follows: In section 2 the methods are presented. The model’s hydrography and circulation are evaluated in sections 3.1 and 3.2, and the relationships between the two are discussed in sections 3.3 and 3.4. Finally, the paper is summarized in section 4.

2. Methods

[6] The model used is a nested version of the Miami Isopycnic Coordinate Ocean Model (MICOM) [Bleck *et al.*, 1992], set up for the Nordic seas and the northern North Atlantic (Figure 1). The nested model is initialized with interpolated model data from a global derivative of MICOM [Bentsen *et al.*, 2004; Furevik *et al.*, 2003; Nilsen *et al.*, 2003]. The global model has a resolution of about 40 km over most of the North Atlantic, whereas the nested model has twice that resolution. Otherwise the grid configurations of the models are identical. The nesting approach applies a boundary relaxation scheme toward the outer (i.e., global) solution. This results in a so-called one-way nesting where the boundary conditions of the nested model are relaxed toward the output from the global model. For the slowly varying baroclinic velocity, temperature, salinity and layer interface variables, this is a fully appropriate way to include the boundary conditions. For the barotropic variables, the relaxation approach requires careful tuning to avoid reflection of waves at the open boundaries. The nested model reads the global fields once a week and interpolates in time to specify the relaxation boundary conditions at each time step. In the vertical, both model versions have 26 layers of which the uppermost layer has temporal and spatial varying density, and the 25 layers below have constant density.

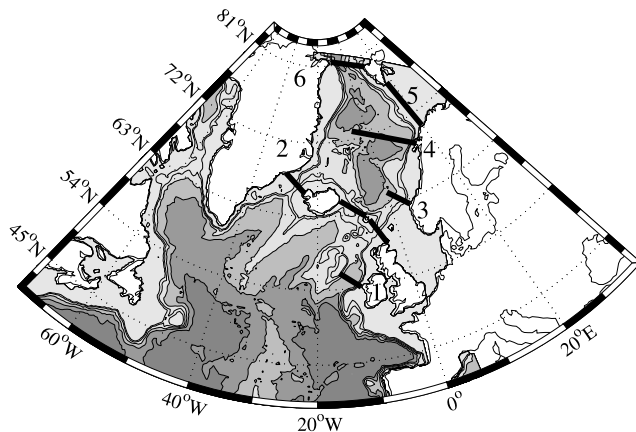


Figure 1. Map of the northern North Atlantic, including the Nordic seas. Topography is shaded within the model domain, and bottom contours are drawn for 500, 1000, 2000, 3000, 4000, and 8000 m. Thick lines show sections for calculation of model fluxes and mean values of salinity, temperature, and density. 1, Rockall; 2, Greenland-Scotland Ridge (GSR); 3, Svinøy; 4, Gimsøy; 5, Barents Sea opening; 6, Fram Strait.

[7] In the nested model, daily NCEP/NCAR reanalysis [Kistler *et al.*, 2001] fresh water, heat and momentum fluxes are used to force the system by applying the scheme of Bentsen and Drange [2000]. If the model sea surface state is about equal to the assumed sea surface state of the NCEP/NCAR reanalysis data, the turbulent fluxes of momentum and heat are estimated by the atmospheric model, which provides the reanalysis data. This model uses bulk expressions to estimate the turbulent fluxes with the coefficients determined by Miyakoda and Sirutis [1986]. If the sea surface state differs significantly between the ocean model and the reanalysis data, the fluxes are modified.

[8] Mixed layer temperature and salinity fields are linearly relaxed toward the monthly mean climatological values of Levitus *et al.* [1994] and Levitus and Boyer [1994], respectively. The e-folding relaxation timescale is set to 30 days for a 50-m-thick mixed layer, and the relaxation is reduced linearly when the mixed layer depth exceeds 50 m. In addition, the relaxation is limited to a maximum difference between the observed and simulated sea surface salinity of 0.5 psu, and the observed and simulated sea surface temperature of 1.5°C. This constraint ensures that the hydrography in regions with large model biases, such as the region of the separation of the Gulf Stream system, is not destroyed by the applied relaxation. This all means that if no other forces or changes act on the waters, they would approach the relaxation target (i.e., monthly mean) salinity or temperature fields by a factor of 1/e after 30 days. However, the ocean surface waters are exposed to exchanges with surrounding waters and to daily atmospheric forcing in this period, so the effect of the relaxation will tend to be masked by atmospheric forcing, ocean transport and mixing processes.

[9] Realistic runoff is incorporated through the NCEP/NCAR reanalysis data and the Total Runoff Integrating Pathways (TRIP) database [Oki and Sud, 1998], and the model is coupled to a sea-ice module consisting of the

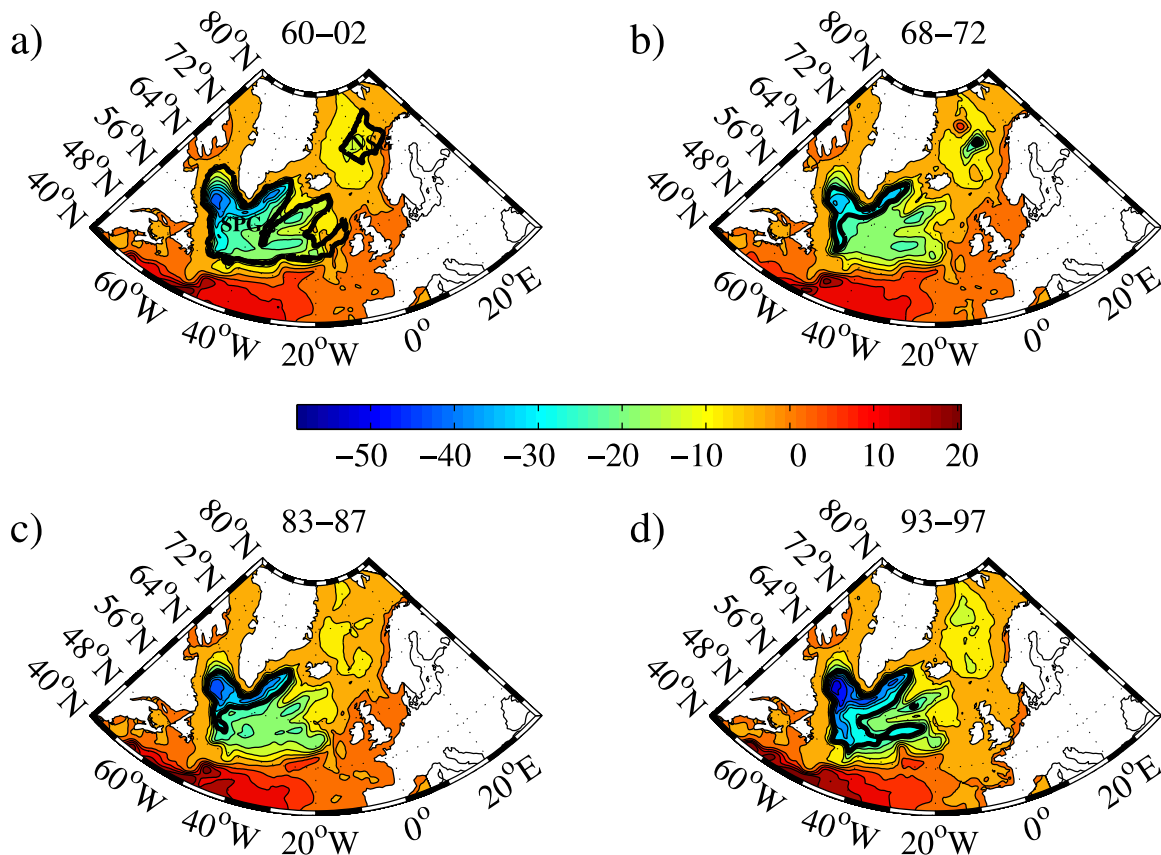


Figure 2. Upper 1000 m vertically integrated stream function (Sv), averaged for the period (a) 1960–2002, (b) 1968–1972, (c) 1983–1987, and (d) 1993–1997. Also shown in Figure 2a are the Subpolar Gyre (SPG) and Nordic Seas Gyre (NSG). The Subpolar Gyre is defined by the 2000-m isobath, except in south, where the mean position of the -12 -Sv stream function contour forms the boundary. The Nordic Seas Gyre is defined as within the 2000-m isobath and two straight lines between Jan Mayen ($71^{\circ}\text{N}, 8^{\circ}\text{W}$) and Spitsbergen ($76^{\circ}\text{N}, 16^{\circ}\text{E}$) or Halten Bank ($68^{\circ}\text{N}, 2^{\circ}\text{E}$). Contour interval is 5 Sv. In Figures 2b–2d, the Subpolar Gyre core size is indicated by highlighting the -24 -Sv contour.

Hibler [1979] rheology in the implementation of Harder [1996] and the thermodynamics of Drange and Simonsen [1996]. Further description of the model is given by Sandø and Drange [2006] and Hátún et al. [2005a].

[10] The large-scale horizontal circulation is analyzed in terms of the vertically integrated stream function (Figure 2). We calculate the volume-weighted average temperature and salinity, as well as total heat and freshwater content, in the upper 1000 m of the gyres, and calculate the different contents within each gyre as a function of time without correcting for volumetric changes. (Heat content $H = \int c_p \rho_w (\theta - \theta_r) dz$ and freshwater content $F = \int (S_r - S)/S_r dz$, where $c_p = 3990 \text{ J kg}^{-1} \text{ K}^{-1}$, $\rho_w = 1020 \text{ kg m}^{-3}$, θ potential temperature, S salinity, $\theta_r = \theta_{1959-2002}$ and $S_r = S_{1959-2002}$ (i.e., averaged over the 1959–2002 period).) The Subpolar Gyre is defined by the 2000-m isobath, except in the south, where the mean position of the -12 -Sv stream function contour forms the boundary. We also calculate the size of the core of the Subpolar Gyre, because it is obvious that the core of the gyre contracts and expands significantly over time (Figure 2). To quantify that feature, we calculate the area within a given stream function, here chosen as -24 Sv.

[11] Changes in the Meridional Overturning Circulation are often studied by exploring the time variability of the maximum overturning in the North Atlantic (typically found at 40°N – 50°N). This study is focusing on the variability at 60°N – 65°N , where one third of the total MOC enters the Nordic seas across the Greenland-Scotland Ridge. Because the flow of light and dense water masses at these latitudes often are found in the same depth range, we find it necessary to use a combination of temperature and density, rather than a depth interface, to differentiate between the northward flowing warm water and the southward flowing cold and dense waters. In particular, we define the Norwegian Atlantic Current in terms of density and temperature, and calculate volume, temperature and salinity transports, as well as area-weighted temperatures and salinities of the Norwegian Atlantic Current for various sections along the coast of Norway (see Figure 1 and Table 1). In general we differentiate between warm Atlantic waters, cold Polar waters and dense overflows at the Greenland-Scotland Ridge.

[12] All time series analyzed are annual means for the period 1959–2002 (the model itself was run for the period 1950–2002), and conclusions drawn are based on the

Table 1. Water Mass Definitions Used in Transport Calculations^a

Section Name	Water Mass Definitions	Mean Transport			Mean	
		Volume, Sv	Heat, TW	Salt, kT/s	S, psu	θ , °C
Rockall (1)	Atlantic Water $\sigma_\theta \leq 27.38 \text{ kgm}^{-3}$	6.1	234	221	35.28	9.7
Iceland-Faroe	Atlantic Water $\sigma_\theta \leq 27.77 \text{ kgm}^{-3}$ $\theta > 2^\circ\text{C}$	2.6	75	90	35.05	7.1
Faroe-Scotland	Atlantic Water $\sigma_\theta \leq 27.77 \text{ kgm}^{-3}$ $\theta > 2^\circ\text{C}$	3.8	142	139	35.22	8.5
Svinøy (3)	Atlantic Water $\sigma_\theta \leq 27.77 \text{ kgm}^{-3}$ $\theta > 2^\circ\text{C}$	6.6	199	245	35.01	6.9
Gimsøy (4)	Atlantic Water $\sigma_\theta \leq 27.77 \text{ kgm}^{-3}$ $\theta > 2^\circ\text{C}$	7.1	179	258	34.93	5.9
Barents Sea opening (5)	Atlantic Water $\sigma_\theta \leq 27.77 \text{ kgm}^{-3}$ $\theta > 2^\circ\text{C}$	2.8	55	109	34.87	4.3
Fram Strait (6)	Modified Atlantic Water $\sigma_\theta \leq 27.98 \text{ kgm}^{-3}$ $\theta > 0^\circ\text{C}$	-0.5	-2	-18	34.81	0.7
Greenland-Scotland Ridge (2)	Atlantic Water $\sigma_\theta \leq 27.77 \text{ kgm}^{-3}$ $\theta > 2^\circ\text{C}$	6.7	224	241	35.01	7.4
Greenland-Scotland Ridge (2)	Light Polar Water $\sigma_\theta \leq 27.77 \text{ kgm}^{-3}$ $\theta \leq 2^\circ\text{C}$	-2.8	-13	-96	34.08	-1.2
Greenland-Scotland Ridge (2)	Dense Overflow Water $\sigma_\theta > 27.77 \text{ kgm}^{-3}$ $\theta \leq 2^\circ\text{C}$	-2.3	-3	-81	34.80	-0.2

^aMean values (1959–2002) of volume, heat and salt transport, and temperature and salinity in the Atlantic Water mass layers of sections 1–6 in Figure 1. For section 2, the Greenland-Scotland Ridge, mean values for the cold out-flowing water mass layers also are shown. The section is divided into the Iceland-Faroe and Faroe-Scotland part as well. Here σ_θ is potential density, T is temperature, and S is salinity. Transport is net transport, directed northward, and 1 Sv = $10^6 \text{ m}^3/\text{s}$.

occurrence of significant correlation coefficients between detrended time series. In calculating significance levels for correlations, the effective number of independent observations, adjusted for order 1 and 2 autocorrelations (N_e) were estimated by the formula of *Quenouille* [1952]: $N_e = N / (1 + 2 r_a^1 r_b^1 + 2 r_a^2 r_b^2)$, where N is the number of data points in the two series (i.e., 43), r_a^1 and r_b^1 are the lag-one autocorrelations, r_a^2 and r_b^2 the lag-two autocorrelations. It is important to bear in mind that high correlation between two parameters can be due to either a close relationship between them or their simultaneous dependence on a third variable. Therefore any given correlation is only meaningful if it supports a scientific hypothesis.

3. Results

3.1. Hydrography

[13] The model has been evaluated against observed temperature [*Hátún et al.*, 2005a] and salinity [*Hátún et al.*, 2005b] at various locations near the Greenland-Scotland Ridge. In the work by *Hátún et al.* [2005a] temperature observations from two different sections in the Faroe-Shetland Channel [*Turrell et al.*, 2003] were merged to produce a century-long hydrography time series. The correlation between the 195 raw temperature observations and the corresponding simulated temperature is was 0.93 without low-pass filtering, and 0.63 when annual averages were used. In addition, daily sea surface temperature measurements from Mykines on the southwestern tip of the Faroes are available for the period 1 January 1914 to 18 September 1969. The correlation between the Mykines series and the simulated temperature anomalies on the Faroe Shelf was 0.96, and 0.75 when monthly averages were used. *Hátún et al.* [2005a] therefore demonstrate that both the simulated seasonal and interannual temperature variations on the Faroe Plateau are realistically captured by the model. In addition, the model simulates the observed changes in seasonal temperature variation both with respect to amplitude and phase. Therefore *Hátún et al.* [2005a] demonstrate that the model is fully capable of simulating the interannual variability of the temperatures despite the applied temperature relaxation.

[14] The same conclusion holds for interannual to decadal-scale variability of surface water salinity [*Hátún et al.*,

2005b]. In this study, observed and simulated salinities were compared in the Rockall Through, in the Irminger Sea and north of the Faroes. For all time series, a close match between the observed and simulated time series were obtained, again illustrating that the applied relaxation does not dampen hydrographic anomalies.

[15] Finally, time series of the simulated top-to-bottom freshwater storage anomalies in the subpolar basins southward to 50°N show very similar freshening trend and interannual variability to that reported in observations [*Curry and Mauritzen*, 2005] for the last 40 years (Figure 3).

3.2. General Circulation

3.2.1. General Circulation: Horizontal Gyres

[16] The large-scale model circulation is dominated by horizontal, cyclonic, gyres. The Subpolar Gyre has an average circulation strength of 40 Sv, whereas the Nordic Seas Gyre has an average strength of 15 Sv (Figure 2a). During the 50-year model simulation the circulation strength varies substantially. The Subpolar Gyre reaches a minimum in early 1970, when the strength averaged ~ 35 Sv for 5 years (Figure 2b, core of gyre indicated by the thick contour line) and a maximum in 1994 of over 55 Sv (Figure 2d). This evolution in circulation strength is consistent, both qualitatively and quantitatively, with the transport index calculated by *Curry and McCartney* [2001], based on potential energy differences between the subpolar and subtropical gyres. The Nordic Seas Gyre reached a maximum of over 30 Sv in the early 1970s (Figure 2b) and a minimum of less than 10 Sv in the 1980s (Figure 2c). The amplitude of the variability in the gyres can thus be well over 50%. The size (defined as above), in particular of the Subpolar Gyre, varies proportionally to the strength; a weaker Subpolar Gyre, such as around 1970, is narrower than a strong one, such as around 1995 (Figures 2b and 2d); thus the circulation strength changes are reflected in circulation pathway changes as well.

3.2.2. General Circulation: Inflow of Warm Atlantic Water to the Nordic Seas

[17] The MOC, bringing warm water northward and dense, cold water southward, is small in comparison to the gyres: At the southern boundary of the domain (30°N ; where the MOC of the global model is imposed) the MOC strength is roughly 18 Sv, and at the Greenland-Scotland

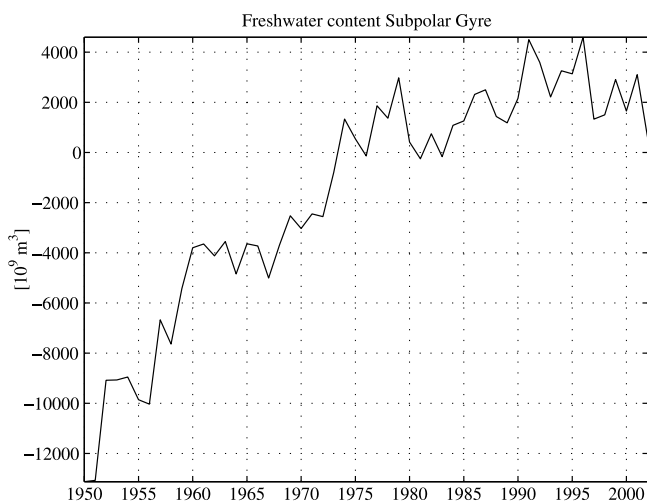


Figure 3. Time series of top-to-bottom freshwater content anomaly (10^3 km^3), relative to the 1959–2002 period, in the Subpolar Gyre, as defined in Figure 2a.

Ridge the inflow of warm water to the Nordic seas (defined as in Table 1) is on average between 6 and 7 Sv. The inflow of warm Atlantic Water at the Greenland-Scotland Ridge is distributed between the branch west and east of the Faroes: the Iceland-Faroe section carries roughly 2.5 Sv, and the Faroe-Scotland section carries nearly 4 Sv. The contribution to the total inflow from the Irminger Current west of Iceland is small in comparison to the other two branches. These numbers are all consistent with observational evidence, which suggests that on average the former two branches carry around 3.5 Sv each, and the latter carries about one eighth of the total inflow [Kristmannsson, 1998; Hansen and Østerhus, 2000].

[18] The model time variability of the exchange across ridge (Figure 4) is also less than that of the gyres: The warm-water inflow exhibits a minimum of 6 Sv in the mid-1960s followed by a maximum of 7.5 Sv in the early 1970s. Then the time series exhibits an all-time low of 5.5 Sv in 1980 and another maximum of 7.5 Sv around 1990. In relative terms, the variability of the northward flow of warm water across the Greenland-Scotland Ridge is roughly 15% of the mean.

3.2.3. General Circulation: Return Flow to the North Atlantic

[19] The export of cold water back to the North Atlantic across the Greenland-Scotland Ridge is divided between dense waters overflowing the ridge and a flow of lighter Polar waters (defined as in Table 1). The dense overflow average about 2.3 Sv (Figure 4), and the light polar waters, which return to the Atlantic in the same light density range as the northward flowing warm water, although much colder and much fresher, are generally as strong or stronger than that of the dense overflows (Figure 4). Comparing the model to the range of observations made on the Greenland-Scotland Ridge (see summaries by Hansen and Østerhus [2000] and McCartney and Mauritzen [2001]) it is clear that the model underestimates the strength of the dense overflows (compare the modeled 2.3 Sv to the observed ~ 5 Sv [Dickson and Brown, 1994]). The long-term average of the light outflows

is less well known; Hansen and Østerhus [2000] present numbers ranging from 1.3 Sv to 3 Sv, so the model's average 2.8 Sv is within the range of possibilities.

[20] Both in the model and in the real world, there is an imbalance in the volume flux across the Greenland-Scotland Ridge. This is possible because the system is not closed: It opens to the Arctic, and therefore to the Pacific Ocean through the Bering Strait and to the Labrador Sea through the Canadian Archipelago. Observations at the Bering Strait indicate a 0.8 Sv net inflow from the Pacific to the Arctic Ocean [Woodgate and Aagaard, 2005]. The net southward flow through the Canadian Archipelago is recently estimated to be 2 Sv [Prinsenbergh and Hamilton, 2005]. To be consistent with these observations, there must be a net northward flow through the Nordic seas, i.e., an imbalance between the northward and southward flow at the Greenland-Scotland Ridge, of roughly 1 Sv. This imbalance may be exaggerated in the model, because of the underestimation of the dense overflows.

[21] During the 50-year simulation period the dense overflows varies by 20–30% on interannual timescales (Figure 4). There does not exist a significant relationship between the variability of the warm inflow and of the dense overflows. However, the light outflows (polar waters of the East Greenland Current) are strongly correlated with the warm inflow, with no time difference (Figure 4). To summarize, owing to the Arctic throughflow, there does not exist a one-to-one relationship between the strength of the northward flowing warm water and the southward flowing cold water across the Greenland-Scotland Ridge.

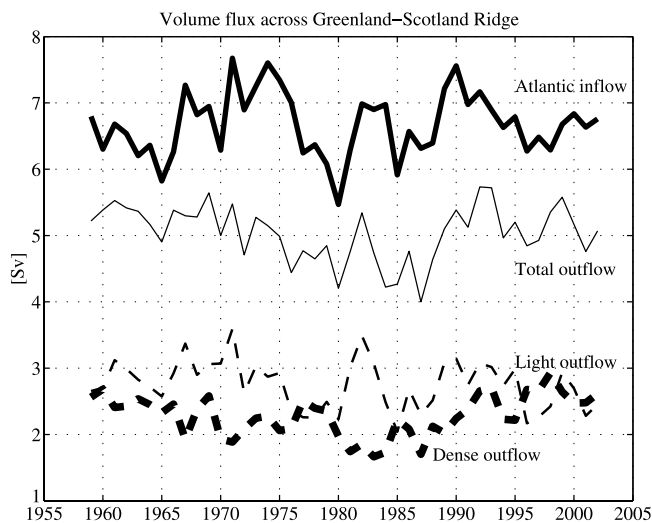


Figure 4. Time series of volumetric exchange across Greenland-Scotland Ridge. The section is indicated in Figure 1. The thick solid line shows northward transport of Atlantic Water (positive northward), defined as water warmer than 2°C and with potential density (σ_0) less than or equal to 27.77 kg/m^3 . The thick stippled line is dense overflow ($\sigma_0 > 27.77 \text{ kg/m}^3$; $\theta \leq 2^\circ\text{C}$), thin stippled cold, light outflow ($\sigma_0 \leq 27.77 \text{ kg/m}^3$; $\theta \leq 2^\circ\text{C}$). The thin solid line is the sum of the two latter, and represents the sum of all southward flow across the Greenland-Scotland Ridge. The imbalance between the thick and thin solid lines represents northward flow into the Arctic.

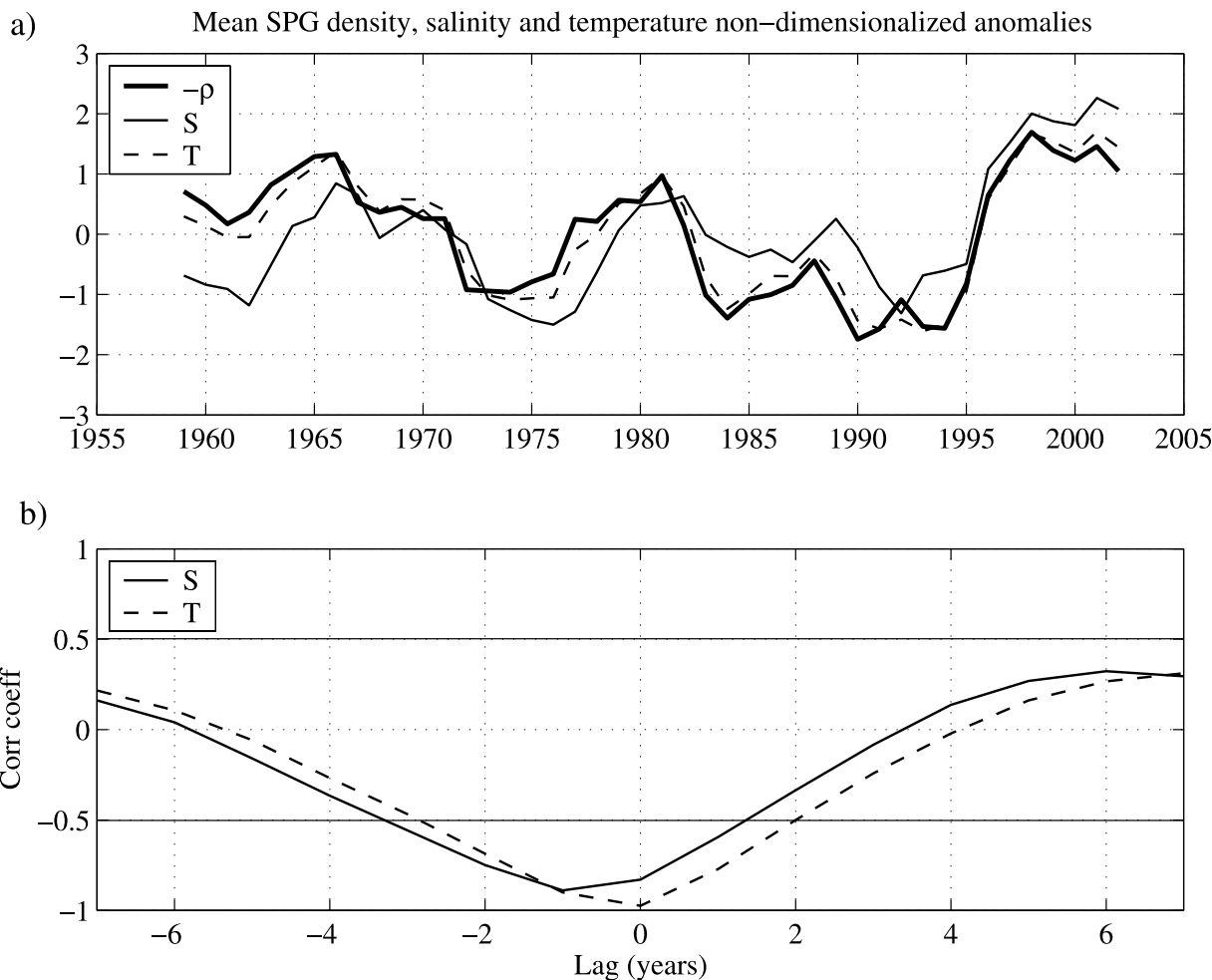


Figure 5. (a) Time series of nondimensionalized average potential density anomaly (thick solid line), average salinity anomaly (thin solid line), and average temperature anomaly (dashed line) in the Subpolar Gyre. Note that density anomaly is inverted. (b) Correlations of density versus salinity (solid line) and density versus temperature (dashed line). Significance levels for the two curves are calculated separately [Quenouille, 1952], and may differ slightly. For simplicity, only the lowest value (strongest criteria for significance) is plotted (horizontal lines). Thus values between the lines are not significant. Negative time lag indicates that the first variable (here: potential density anomaly) leads the others (here: salinity and temperature anomalies). All time series are detrended before correlation.

In the model, variability in the warm inflow is strongly correlated ($r = -0.62$) with variability in the outflow of cold and light polar waters. No such relationship is found for the dense overflows. We cannot confirm whether this finding is robust, owing to the underestimation of the strength of the dense overflows. We do, however, find the result to be sensible, and it points to a possible decoupling of the upper limb of the MOC from the lower.

3.3. Hydrography and Circulation

3.3.1. Hydrography and Circulation: Subpolar Gyre

[22] The time evolution of the freshwater content of the Subpolar Gyre is quite different if one considers only the upper part of the gyre rather than the full depth (which was discussed in section 3.1). In the upper part of the water column the salinity is characterized by interannual to decadal variability and a monotonic reduction of the fresh-

water content during the 1990s toward the saltiest waters of the simulation period (Figure 5; here the upper 1000 m is used, but the finding is the same for the upper 200 m or 500 m). In particular, the observed salinity anomalies of the 1970s, 1980s and early 1990s in the Subpolar Gyre (see section 1) are reproduced.

[23] The salinity anomalies are covarying with temperature anomalies, such that when the Subpolar Gyre is fresh, it is also cold (Figure 5). However, even though they affect density oppositely, the density does not remain constant. Instead, the density follows the temperature evolution, giving the counterintuitive result that when the Subpolar Gyre is fresh, it is also dense (Figure 5). Observations from weather ship *Bravo* in the western Subpolar Gyre show the same result [Curry and McCartney, 2001].

[24] Comparing the hydrography of the Subpolar Gyre to the circulation, we find increased strength of the Subpolar

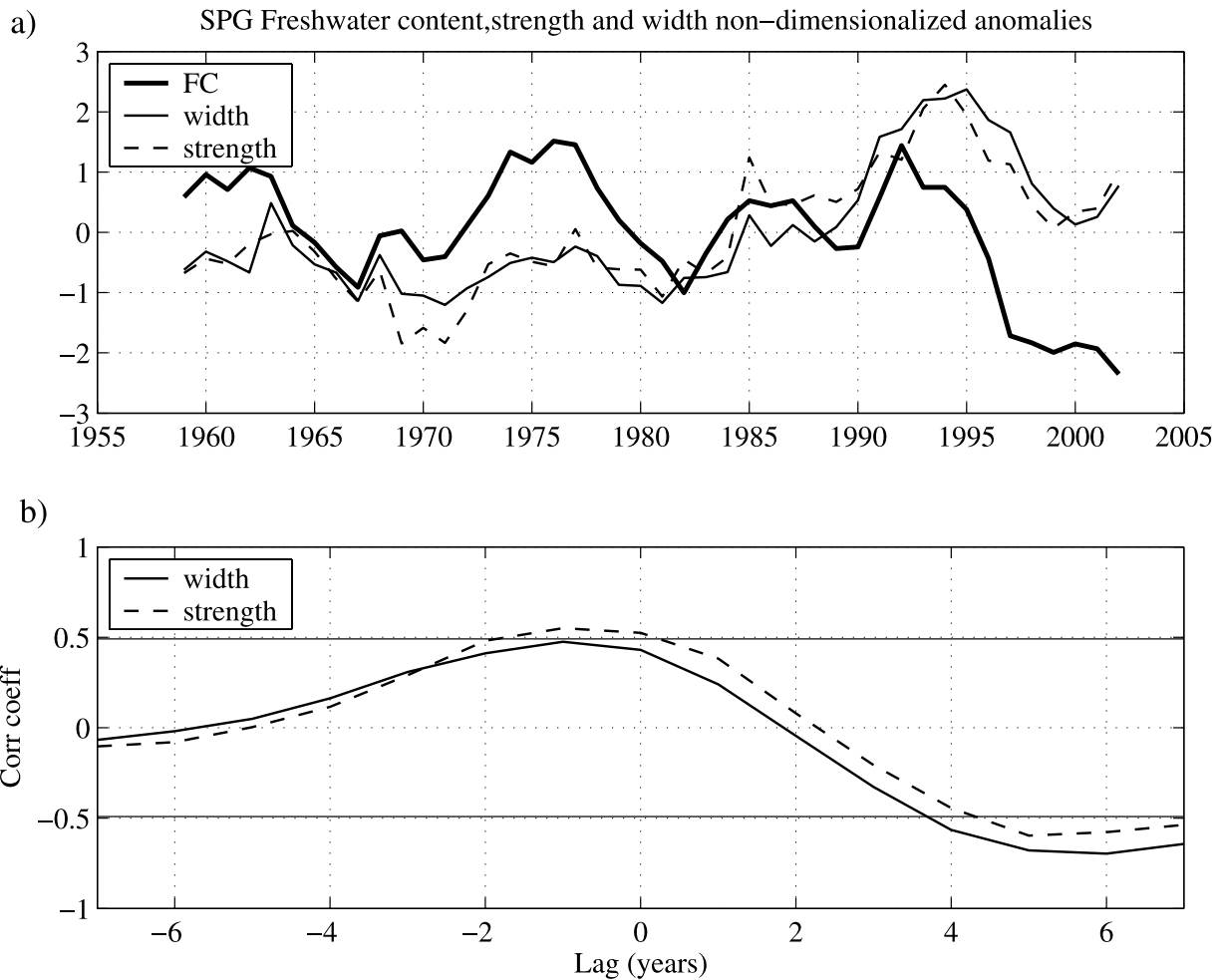


Figure 6. (a) Time series of nondimensionalized upper 1000-m freshwater content anomaly (FC) (thick solid line), gyre width anomaly (thin solid line), and gyre strength anomaly (dashed line) in the Subpolar Gyre. (b) Correlations of freshwater content versus gyre width (solid line) and freshwater content versus gyre strength (dashed line). Otherwise as in Figure 5.

Gyre occurring during the periods of the “great salinity anomalies” (Figure 6). Specifically, these hydrographic anomalies are precursors of gyre circulation changes: About 1 year after the freshwater content of the Subpolar Gyre goes up the gyre strength and width increases (Figure 6). We also note a second correlation: Five years after the gyre strength and width goes up the freshwater content returns to normal. This points to an oscillatory nature of the phenomenon. Whereas the former correlation is limited to the upper waters, the latter is representative of the entire water column.

[25] Can we establish a physical connection between these processes? *Eden and Willebrand [2001]* investigate the dynamic response of the Subpolar Gyre to atmospheric forcing, and describe it as a two-step process: First there is an immediate, barotropic, response (slowing down the gyre in the case of high NAO) driven by the winds alone, and then there is a delayed response (roughly 3-year lag time, speeding up the gyre in the case of high NAO) due to a combination of the wind and buoyancy forcing. *Curry and McCartney [2001]* emphasize the connection between the

winter North Atlantic Oscillation index (NAO) and their baroclinic index of transport strength between the Subtropical and Subpolar Gyres; specifically, they show the evolution from a low transport state in the 1970s to a high in the early 1990s. *Häkkinen and Rhines [2004]* show observational evidence for the decline in Subpolar Gyre strength in the 1990s (also seen in the model simulation, Figure 6) and relate it to changes in the buoyancy forcing over the Subpolar Gyre. Therefore it is reasonable to hypothesize that the variability we have found in hydrography and circulation on interannual to decadal timescale is related to atmospheric forcing.

[26] For simplicity, we use the NAO index (specifically the December–March principal component based NAO data provided by the Climate Analysis Section, NCAR, Boulder [see *Hurrell, 1995*]) as a proxy for the large-scale atmospheric forcing. We could have picked a more sophisticated measure, but we believe the connections are well enough established through the use of the NAO. We find that an NAO increase is followed in the model by hydrographic changes (cooling, due to the increased oceanic heat

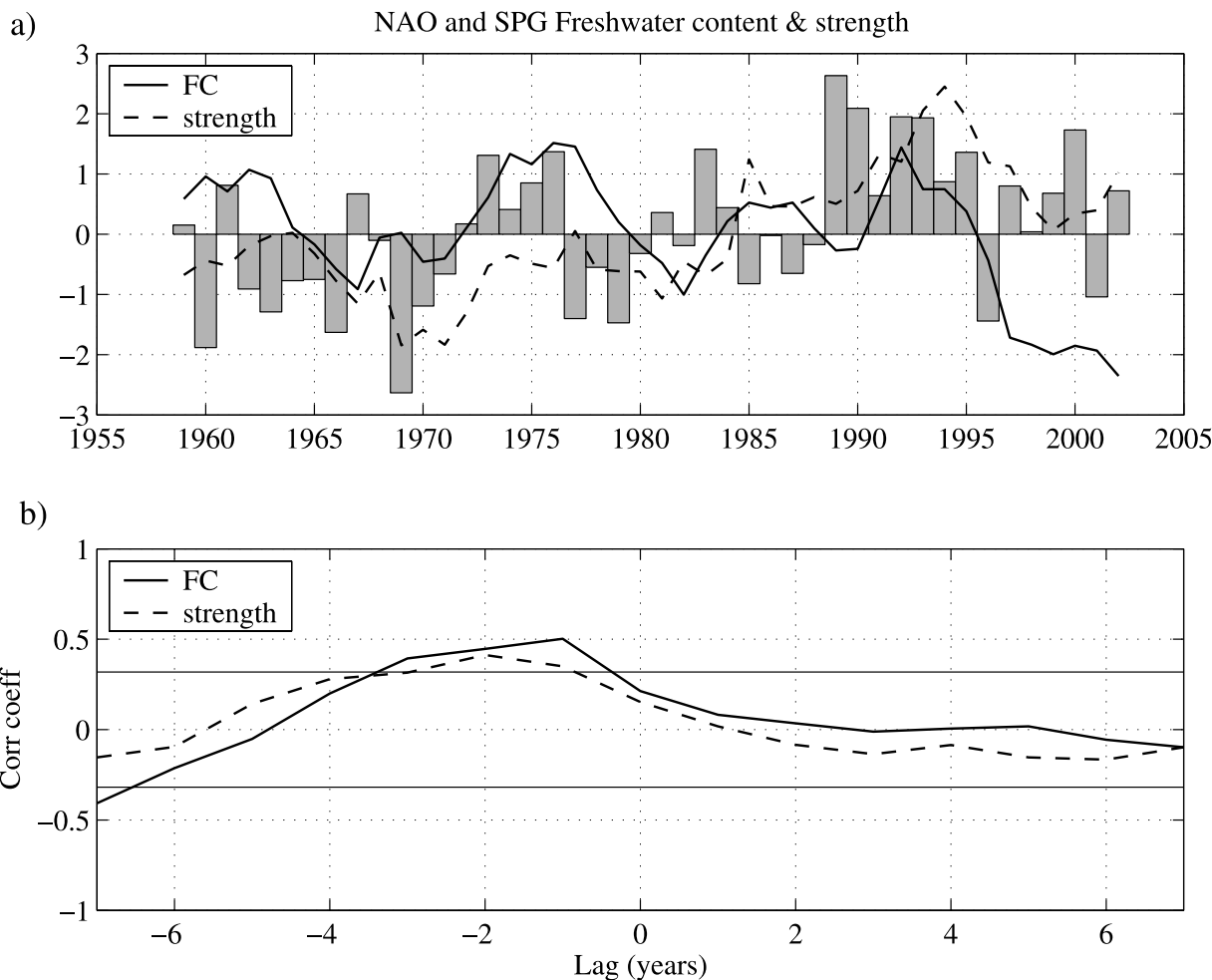


Figure 7. (a) Time series of NAO index, nondimensionalized freshwater content anomaly (solid line) and gyre strength anomaly (dashed line) in the Subpolar Gyre. (b) Correlations of NAO versus freshwater content (solid line) and NAO versus gyre strength (dashed line). Otherwise as in Figure 5.

losses as more cold continental air reaches the western Subpolar Gyre, and freshening, due to increased freshwater export from the Arctic) in the upper waters of the Subpolar Gyre after about 1 year, by a strengthening and widening out of the Subpolar Gyre after 2 to 3 years, and, finally, by a warming and salinification in the entire water column after 7–8 years (Figures 6 and 7). This last response is not connected to the NAO (see Figure 7), which further suggests that it is symptomatic of an internal, oscillatory, response of the Subpolar Gyre.

[27] In the Subpolar Gyre it is *Eden and Willebrand's* [2001] delayed, rather than immediate, response to the NAO we pick up in our analysis. As we will see in the next section, the model does exhibit an immediate response to the NAO, but it is found in the exchange across the Greenland-Scotland Ridge.

3.3.2. Hydrography and Circulation: Inflow of Atlantic Water to the Nordic Seas

[28] The inflow of Atlantic Water to the Nordic seas across the Greenland-Scotland Ridge is fed by the North Atlantic Current, and draws upon waters both from the Subtropical and Subpolar Gyres. In their seminal paper on

the “Great Salinity Anomaly,” *Dickson et al.* [1988] describe how the anomalies propagate cyclonically from the western Subpolar Gyre toward the Greenland-Scotland Ridge and the Norwegian Atlantic Current. A recent study by *Hátún et al.* [2005b] investigates processes by which these anomalies occur.

[29] At the Greenland-Scotland Ridge, the salinity evolution shows strong resemblance to that in the Subpolar Gyre (Figure 8), consistent with *Dickson et al.'s* [1988] observations. The salinity anomalies of the 1970s, 1980s and early 1990s are present. As in the Subpolar Gyre, the density anomalies at the ridge are controlled by the temperature evolution, not by the salinity (Figure 9). In fact, salinity and temperature show a much stronger decoupling at the ridge than in the Subpolar Gyre (contrast Figures 9 and 5). Thus it follows that there is a clear relationship between the salinity anomalies of the Subpolar Gyre and those at the Greenland-Scotland Ridge (the latter lagging the former by less than a year; Figure 8), whereas the temperature anomalies in the two regions are not significantly correlated (not shown). There is a physical explanation for this: Since temperature is the dynamically active

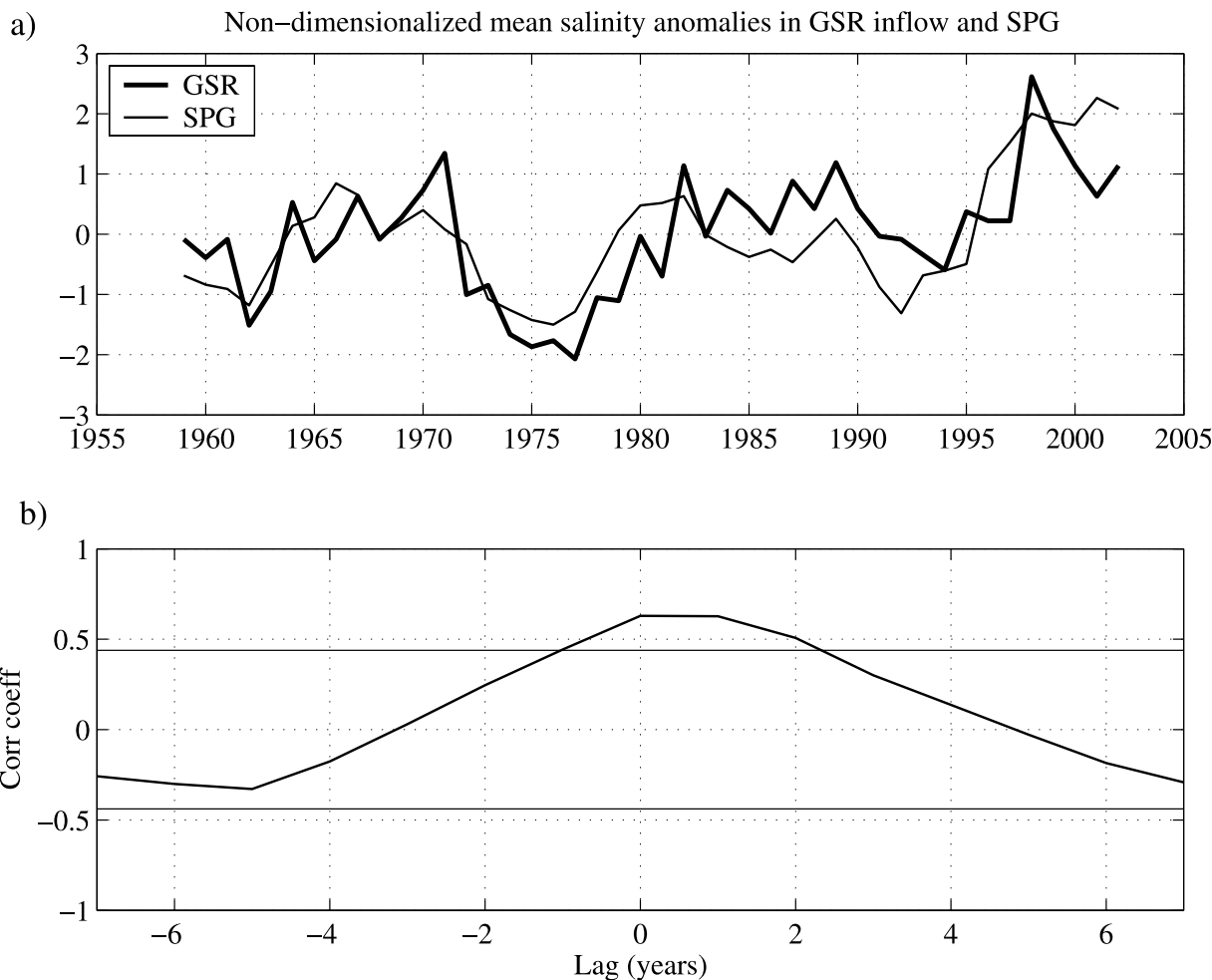


Figure 8. (a) Time series of nondimensionalized average salinity anomaly within the warm water inflow at the Greenland-Scotland Ridge (thick line) and in the Subpolar Gyre (thin line). (b) Correlations of average salinity in inflow versus gyre. Otherwise as in Figure 5.

contributor to the vertical stability of the water column in both places, anomalies in temperature are quickly erased through buoyancy adjustment, whereas salinity anomalies can be passively advected with the general circulation, toward the ridge. These salinity anomalies can therefore maintain some memory of the forcing history.

[30] Following this train of thought one can hypothesize that if there is some relationship between the atmospheric forcing in the Subpolar Gyre and the strength of the inflow of warm Atlantic Water across the Greenland-Scotland Ridge, then there should be a relationship between salinity at the ridge and inflow strength across the ridge. Indeed, this is found in the model: There exists a relationship between salinity and transport strength at the inflow, whereas no such relationship exists between temperature and transport (Figure 10). In the period 2 to 4 years after a transport increase in the inflow the salinity goes down. That is due to the following sequence of events.

[31] 1. The inflow of Atlantic Water to the Nordic seas across the Greenland-Scotland Ridge increases immediately in response to an increase in the NAO, as does the

southward flow of light Polar water across the ridge (Figure 11).

[32] 2. The hydrographic changes develop in the Subpolar Gyre after about 1 year (cooler, fresher, denser; Figure 7). The salinity anomalies advect eastward and appear at the Ridge quickly thereafter (Figure 8).

[33] 3. The Subpolar Gyre starts spinning up and widening out 1–2 years thereafter (Figure 6). These dynamical changes to the Subpolar Gyre are not significantly correlated with the volume transport of warm water into the Nordic seas. They are, however, as we have seen, correlated with the salinities at the ridge, in accordance with *Hátún et al.* [2005b].

[34] Thus salinity is an indicator of circulation change at the Greenland-Scotland Ridge, whereas temperature is not. However, owing to the oscillatory nature of the salinity and inflow strength variability at the ridge (see symmetric correlations for ± 2 –4 years in Figure 10), an oscillatory nature which is not imposed by the forcing (there is no such symmetry in Figure 11), one might claim that the salinity anomalies are indicators of circulation changes both earlier and later in time.

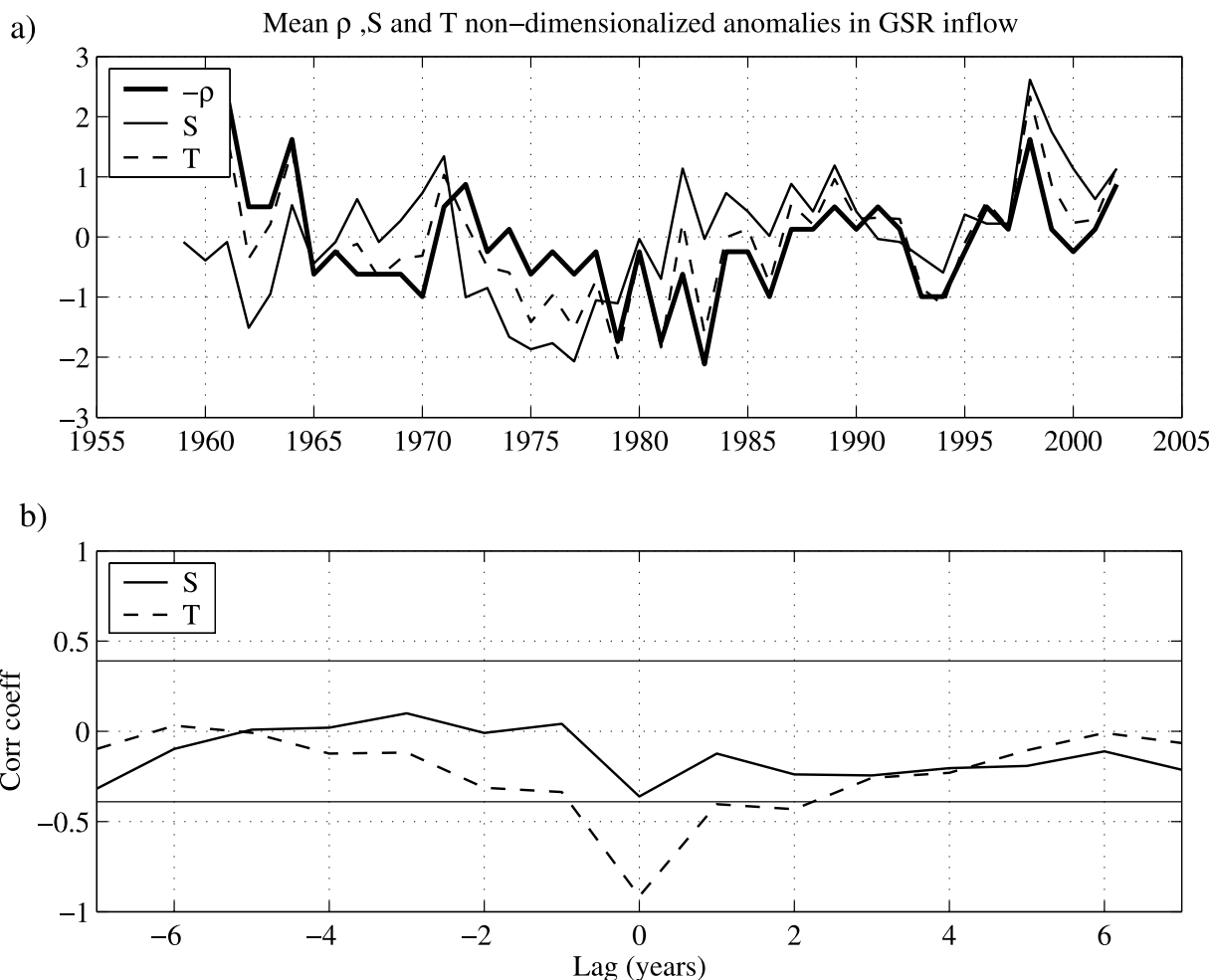


Figure 9. (a) Time series of nondimensionalized average density anomaly (thick solid line), average salinity anomaly (thin solid line), and average temperature anomaly (dashed line) for the warm water inflow at the Greenland-Scotland Ridge. Note that density anomaly is inverted. (b) Correlations of density versus salinity (solid line) and density versus temperature (dashed line). Otherwise as in Figure 5.

3.4. Norwegian Atlantic Current in the Nordic Seas and Toward the Arctic

[35] The flux of temperature into the Nordic seas, which is important for maintaining the heat balance in that region, is generally dominated by the volume flux variability, not the temperature variability. The same is true for salinity. This is true not only for the ridge region, but also for the series of sections along the coast of Norway shown in Figure 1. For all sections along the coast, the correlation values between inflow and salt/temperature fluxes (Figure 12, bottom) are higher than the correlation values between mean salinity/temperature and the same salt/temperature fluxes (Figure 12, top). Observations support this finding: At the Svinøy section (our section 3), analysis of a record 10-year observational time series has shown that on interannual timescales the temperature flux is indeed dominated by the transport variability. It appears that only on longer timescales may temperature variability itself contribute significantly to the temperature flux [Orvik and Skagseth, 2005]. This shows how important it is to monitor

the circulation strength itself, to understand why it may change, and, optimally, to predict these changes.

[36] The equation of state dictates that at lower temperatures, for instance in polar waters, the salinity becomes more and more influential for the density distribution. We see this in the model: As the Atlantic Water flows northward in the Nordic seas and the temperature of the current drops, temperature loses some of its dominance over the density evolution; for instance at the Gimsøy section and at Barents Sea entrance, both temperature and salinity contribute significantly to the density evolution (Figure 13, top). A complete switch to a salinity-controlled density distribution occurs as one reaches the Arctic (see the Fram Strait section in Figure 13, top). Because of this, and quite contrary to most other ocean basins, there exists a subsurface temperature maximum in the Arctic Ocean: the Atlantic layer. Because temperature is not the dynamically active partner in the Arctic, it can be a passive tracer there, following the argument of the previous section. There are indeed numerous observations of temperature anomalies propagating

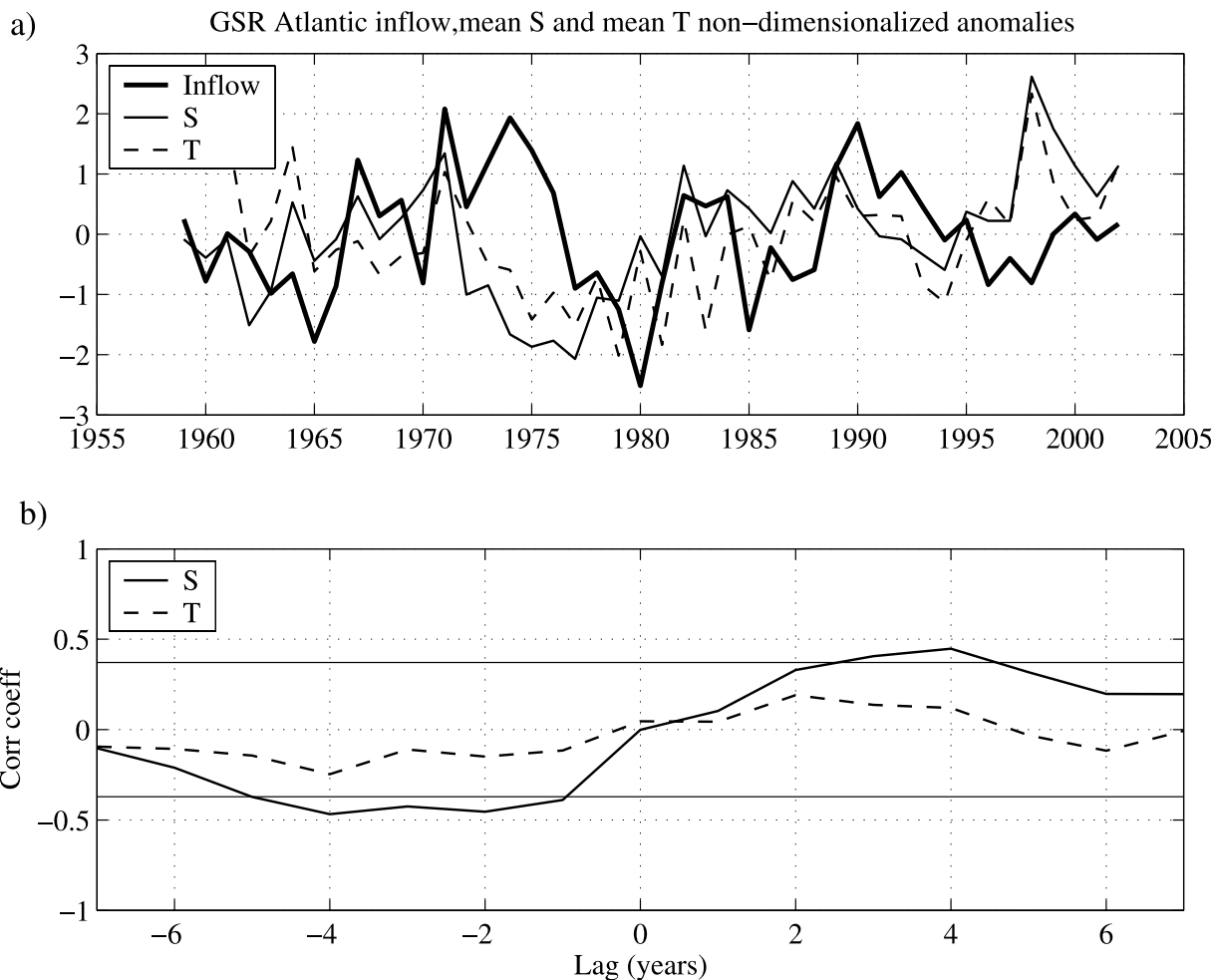


Figure 10. (a) Time series of nondimensionalized volume transport anomaly (thick solid line), average salinity anomaly (thin solid line), and average temperature anomaly (dashed line) for the warm Atlantic Water inflow at the Greenland-Scotland Ridge. (b) Correlations of transport versus salinity (solid line) and transport versus temperature (dashed line). Otherwise as in Figure 5.

cyclonically in the Arctic [see *Quadfasel et al.*, 1991; *Grotefendt et al.*, 1998].

[37] In our model we see indications of a switch from a thermally to a haline-controlled density distribution starting around Gimsøy (Figure 13, top). Following the idea that the passive tracer should carry some information about the forcing history, we should find a similar regime shift in the relationship between circulation and hydrography, and indeed we find a hint of this, albeit weak: South of Gimsøy the correlation between circulation strength and salinity is typically the strongest, whereas at Gimsøy and northward the correlation between circulation strength and temperature is the strongest (Figure 13, bottom). Observations at the Fram Strait entrance to the Arctic support this idea: *Schauer et al.* [2004] find a significant correlation there between a warm and a strong Atlantic Current. We repeat that these are weak correlations, and not always true (notably, at Rockall and the Faroe-Shetland section, temperature is as strong an indicator of circulation change as salinity), but nevertheless they give

yet another hint at what we set out to find: relationships between hydrography and circulation.

4. Summary and Conclusions

[38] With a numerical model we have investigated circulation and hydrography, and the relationship between the two, in the North Atlantic/Nordic seas region, where the northernmost extension of the MOC extends beyond the Atlantic Ocean and continues toward the Arctic. Considering the technological difficulties in monitoring the strength of a current at a variety of locations, it is not surprising that oceanographers seek to find relationships between current strength and oceanic variables that are more easily monitored, such as temperature and salinity. The time span of the simulation is 50 years, which is much too short to suggest robust statistical relationships. Nevertheless, this time span is comparable to the modern observational period; that is, we do not have longer time series in the ocean without going to proxy data. Our findings are supported by a range of observational material, and the scenarios

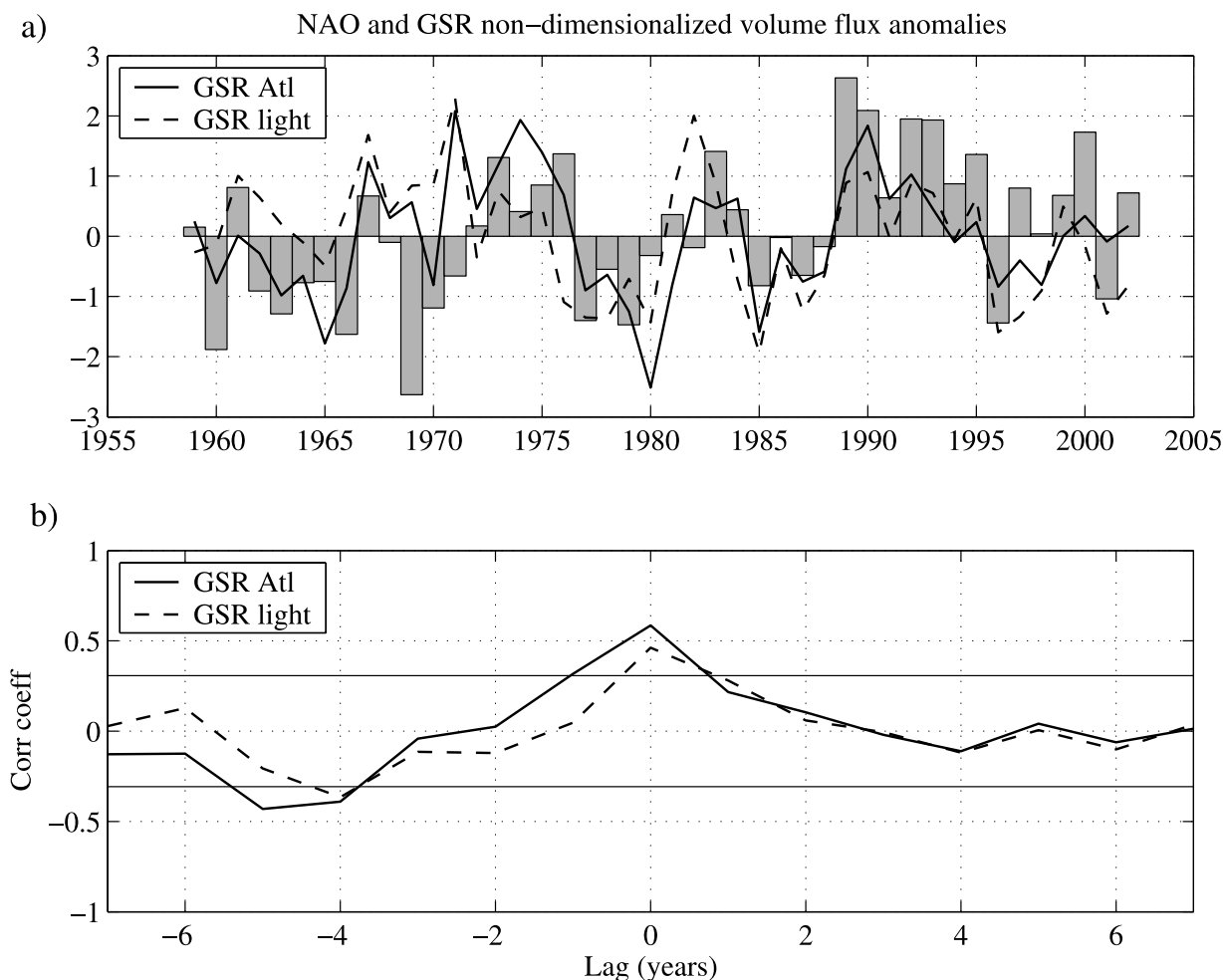


Figure 11. (a) Time series of NAO index, nondimensionalized warm Atlantic Water inflow (solid line) and cold, light Polar Water outflow (dashed line) anomalies at the Greenland-Scotland Ridge. (b) Correlations of NAO versus warm inflow (solid line) and NAO versus Polar outflow (dashed line). Otherwise as in Figure 5.

presented appear consistent. We should emphasize that the variability we have studied is of interannual to decadal nature. Our findings are of a general nature; that is, they will obviously not always hold, not even in the model, but represent the most common occurrences.

[39] We have shown that the northward temperature and salinity flux is controlled by the volume flux rather than the temperature and salinity of the current. We have also seen a connection between that volume flux and the hydrography. This is due to a common denominator: atmospheric forcing. That is, the hydrographic anomalies are indicators of circulation change even though they are not the cause of it. We have established the following sequence of events.

[40] 1. Atmospheric forcing (here condensed into the NAO index) increases in the Atlantic sector.

[41] 2. The inflow of Atlantic Water to the Nordic seas across the Greenland-Scotland Ridge increases immediately, as does the southward flow of light polar water across the ridge.

[42] 3. Hydrographic changes develop in the Subpolar Gyre after about 1 year (fresher, yet denser!). The salinity

anomalies advect eastward and appear at the ridge quickly thereafter.

[43] 4. The Subpolar Gyre starts spinning up and widening out 1–2 years thereafter. However, these dynamical changes to the Subpolar Gyre have become decorrelated from the volume transport of warm water into the Nordic seas.

[44] This all leads to the interesting situation that the salinities of the northward flowing MOC at the Greenland-Scotland Ridge are indicative of circulation strength changes in the northward flow of warm water across the ridge, in retrospect (2–4 years after the circulation change). The salinity anomalies originate in the Subpolar Gyre, and carry information about forcing, the same forcing that caused the circulation changes in the first place, as they propagate toward the ridge area. Owing to a secondary, oscillatory, mode of variability in circulation and salinity at the ridge area the same salinity anomalies are also indicative of upcoming inflow changes (2–4 years later).

[45] Interestingly, even though temperature anomalies are just as prominent in the Subpolar Gyre as salinity anomalies

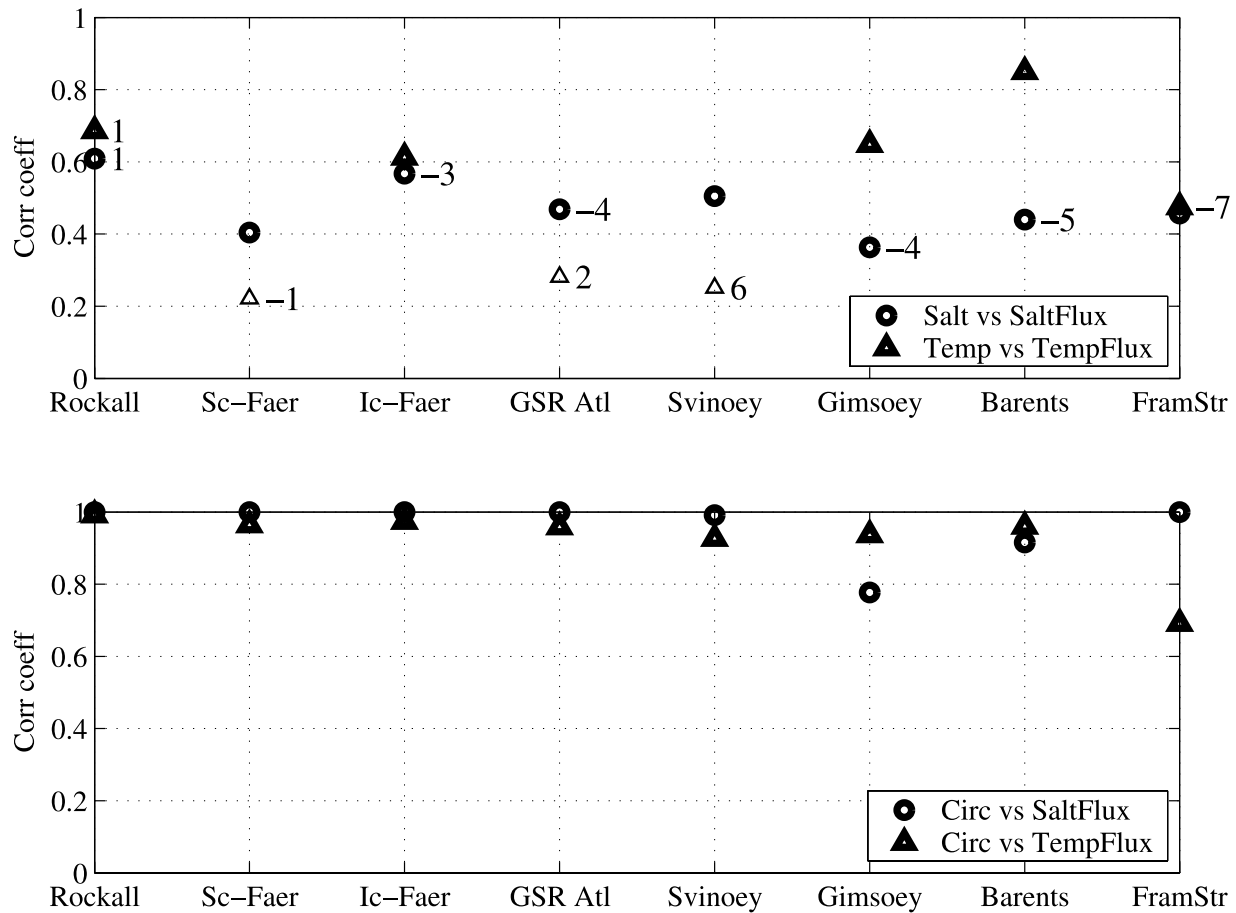


Figure 12. Absolute value of correlation between (top) average salinity and salt flux (circles) or average temperature and temperature flux (triangles) and (bottom) circulation and salt flux (circles) or circulation and temperature flux (triangles). Time lag (years) is indicated at right of symbol if present. Time series are detrended before correlation, and significant values according to *Quenouille* [1952] are shown by bold figures.

are, they do not propagate toward the ridge area. In the hydrographic parameter range of the subpolar North Atlantic, temperature is the dynamically active contributor to density, and anomalies in temperature are therefore likely to be erased through buoyancy adjustment. Salinity, on the other hand, is free to passively advect, as has been observed in the North Atlantic repeatedly. This allows salinity to be an indicator of circulation change as described above.

[46] Within the hydrographic parameter range of the Arctic the situation is the opposite: Salinity is the dynamically active contributor to density. Here temperature can passively advect, as has been observed in the Arctic repeatedly. In the model the transition occurs around 70°N, north of which temperature also is an indicator of circulation change.

[47] Salinity anomalies in the Subpolar Gyre occur owing to local forcing, anomalies in the saline waters entering from the south, and unusually large pulses of freshwater and ice exported from the Arctic. As pointed out by *Curry and McCartney* [2001], even though these freshwater anomalies are dense anomalies, the introduction of freshwater lids can cause a cessation of dense water formation. Looking at the maximum overturning rate of the overturning in the North

Atlantic (AMOC, rather than at the exchange across the Greenland-Scotland Ridge as we do in this paper), *Häkkinen* [1999] finds that its response depends strongly on where, when, and how fast the freshwater lid enters, and can be as large as 20%. *Haak et al.* [2003] find only minor responses in the AMOC as a result of salinity anomalies. *Bentsen et al.* [2004] show that AMOC responds 2–4 years after large (in the sense that both the Labrador and Irminger Seas are involved) variations in the atmospheric forcing. Clearly, hydrographic anomalies play a multitude of roles in the North Atlantic, and in particular for the large circulation system we have come to appreciate as being fundamental to Earth's climate, the MOC.

[48] Finally, our study suggests that it is important to consider the upper and lower limbs of the MOC separately, at least at these high latitudes, owing to the possibilities of light return flows and an exchange through the Canadian Archipelago (at lower latitudes the MOC may not have so many possibilities to disconnect). If one limits the definition of the MOC to that part of the northward flow which is needed to feed the dense return flows, one reduces the problem but loses a significant part of the current that brings warm water northward. European climate, to the extent that

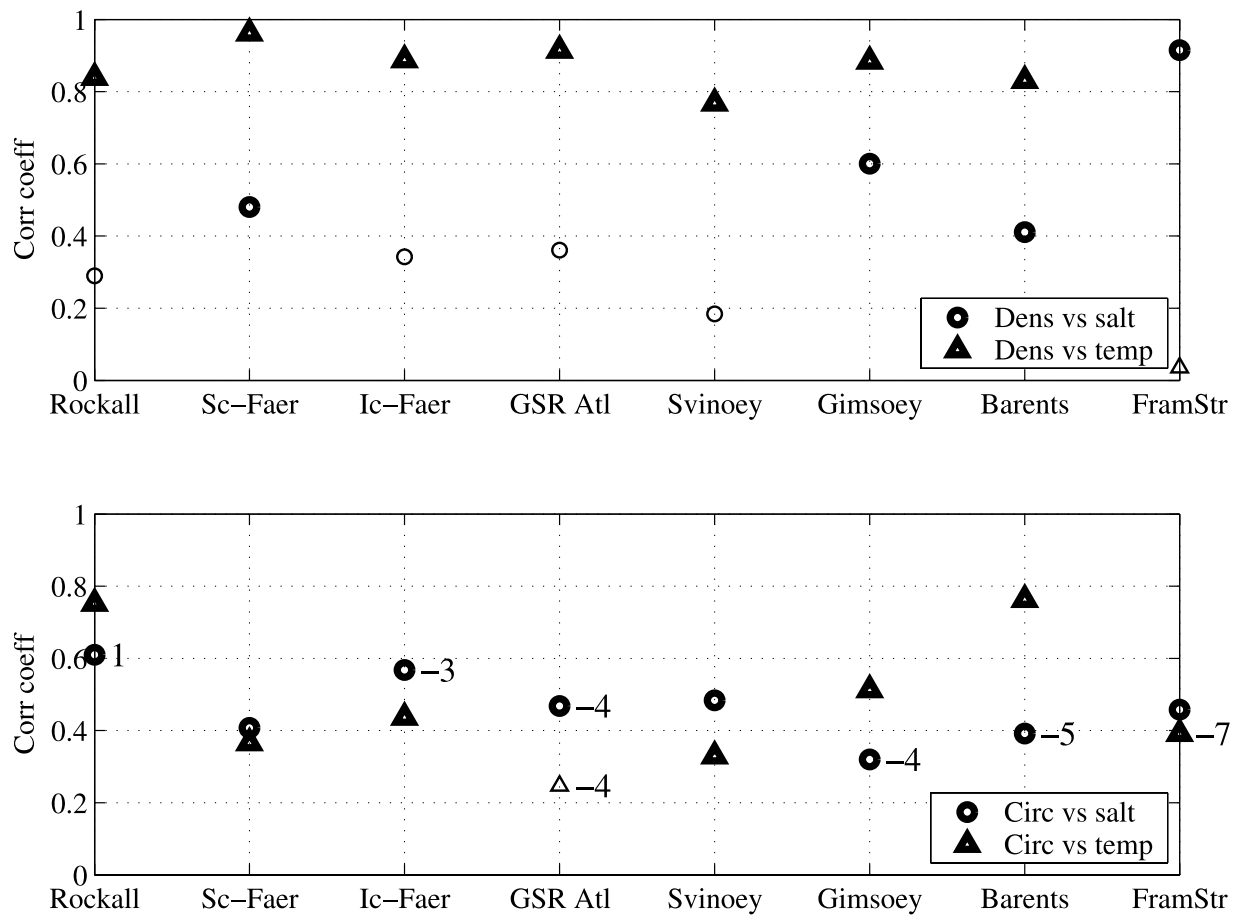


Figure 13. Absolute value of correlation between (a) density and salt (triangles) or temperature (circles) and (b) circulation and salt (triangles) or temperature (circles). Time lag is indicated at right of symbol if present. Time series are detrended before correlation, and significant values according to *Quenouille* [1952] are shown by bold figures.

it is influenced by air-sea heat exchange in Atlantic sector, depends on the upper limb, not the lower limb, of the MOC. The lower limb of the MOC can of course have numerous other impacts on the dynamical couplings between ocean and atmosphere, but those are beyond the scope of this study.

[49] **Acknowledgments.** We gratefully acknowledge the reviewers for their constructive comments. C. M. and S. S. H. acknowledge the support of the Norwegian Research Council through grant 139 815/720 (NOCLimII). A. B. S. acknowledges the support from the Nordic Council of Ministers through a 5-year fellowship related to the West Nordic Ocean Climate Programme. This is publication 3,2006 of the Norwegian Meteorological Institute and publication A130 of the Bjerknes Centre for Climate Research.

References

Belkin, I. M., S. Levitus, J. I. Antonov, and S.-A. Malmberg (1998), "Great Salinity Anomalies" in the North Atlantic, *Prog. Oceanogr.*, *41*, 1–68.

Bentsen, M., and H. Drange (2000), Parameterizing surface fluxes in ocean models using the NCEP/NCAR reanalysis data, *RegClim Gen. Tech. Rep.* 4, pp. 149–158, Norw. Inst. for Air Res., Kjeller, Norway.

Bentsen, M., H. Drange, T. Furevik, and T. Zhou (2004), Simulated variability of the Atlantic meridional overturning circulation, *Clim. Dyn.*, *22*, 701–720.

Bleck, R., C. Rooth, D. Hu, and L. T. Smith (1992), Salinity-driven thermocline transients in a wind- and thermohaline-forced isopycnic coordinate model of the North Atlantic, *J. Phys. Oceanogr.*, *22*, 1486–1505.

Blindheim, J., V. Borovkov, B. Hansen, S.-A. Malmberg, W. R. Turrell, and S. Østerhus (2000), Upper layer cooling and freshening in the Norwegian Sea in relation to atmospheric forcing, *Deep Sea Res., Part I*, *47*, 655–680.

Curry, R., and C. Mauritzen (2005), Dilution of the northern North Atlantic Ocean in recent decades, *Science*, *308*, 1772–1774.

Curry, R. G., and M. S. McCartney (2001), Ocean gyre circulation changes associated with the North Atlantic Oscillation, *J. Phys. Oceanogr.*, *31*, 3374–3400.

Curry, R., B. Dickson, and I. Yashayaev (2003), A change in the freshwater balance of the Atlantic Ocean over the past four decades, *Nature*, *426*, 826–829, doi:10.1038/nature02206.

Dickson, B., I. Yashayaev, J. Meincke, B. Turrell, S. Dye, and J. Holfort (2002), Rapid freshening of the deep North Atlantic Ocean over the past four decades, *Nature*, *416*, 832–837.

Dickson, R. R., and J. Brown (1994), The production of North Atlantic Deep Water, sources, rates, and pathways, *J. Geophys. Res.*, *99*, 12,319–12,341.

Dickson, R. R., J. Meincke, S.-A. Malmberg, and A. J. Lee (1988), The "Great Salinity Anomaly" in the northern North Atlantic, 1968–1982, *Prog. Oceanogr.*, *20*, 103–151.

Drange, H., and K. Simonsen (1996), Formulation of air-sea fluxes in the ESOP2 version of MICOM, *Tech. Rep. 125*, 23 pp., Nansen Environ. and Remote Sens. Cent., Bergen, Norway.

Eden, C., and J. Willebrand (2001), Mechanism of interannual to decadal variability of the North Atlantic circulation, *J. Clim.*, *14*, 2266–2280.

Ewing, M., and W. L. Donn (1956), A theory of ice ages, *Science*, *123*, 1061–1065.

Furevik, T., M. Bentsen, H. Drange, I. K. T. Kindem, G. Kvamstø, and A. Sorteberg (2003), Description and validation of the Bergen Climate Model: ARPEGE coupled with MICOM, *Clim. Dyn.*, *21*, 27–51, doi:10.1007/s00382-003-0317-5.

- Grotefendt, K., K. Logemann, D. Quadfasel, and S. Ronski (1998), Is the Arctic Ocean warming?, *J. Geophys. Res.*, *103*, 27679.
- Haak, H., J. Jungclauss, U. Mikolajewicz, and M. Latif (2003), Formation and propagation of great salinity anomalies, *Geophys. Res. Lett.*, *30*(9), 1473, doi:10.1029/2003GL017065.
- Häkkinen, S. (1999), A simulation of thermohaline effects of a great salinity anomaly, *J. Clim.*, *12*, 1781–1795.
- Häkkinen, S., and P. B. Rhines (2004), Decline of subpolar North Atlantic circulation in the 1990s, *Science*, *304*, 555–559.
- Hansen, B., and S. Østerhus (2000), North Atlantic–Nordic seas exchanges, *Prog. Oceanogr.*, *45*, 109–208.
- Harder, M. (1996), Dynamik, Rauhigkeit und Alter des Meereises in der Arktis, Ph.D. thesis, 124 pp., Alfred-Wegener-Inst. für Polar- und Meeresforsch., Bremerhaven, Germany.
- Hátún, H., A. B. Sandø, H. Drange, and M. Bentsen (2005a), Seasonal to decadal temperature variations in the Faroe-Shetland inflow waters, in *The Nordic Seas: An Integrated Perspective*, *Geophys. Monogr. Ser.*, vol. 158, edited by H. Drange et al., pp. 239–250, AGU, Washington, D. C.
- Hátún, H., B. Hansen, A. B. Sandø, H. Drange, and H. Valdimarsson (2005b), Influence of the Atlantic Subpolar Gyre on the thermohaline circulation, *Science*, *309*, 1841–1844.
- Hibler, W. D. (1979), A dynamic thermodynamic sea ice model, *J. Phys. Oceanogr.*, *9*, 815–846.
- Hurrell, J. (1995), Decadal trends in the North Atlantic Oscillation: Regional temperatures and precipitation, *Science*, *269*, 676–679.
- Kistler, R., et al. (2001), The NCEP–NCAR 50–Year reanalysis, monthly means, CD-ROM and documentation, *Bull. Am. Meteorol. Soc.*, *82*, 247–268.
- Kristmannsson, S. S. (1998), Flow of Atlantic Water into the northern Icelandic shelf area, 1985–1989, *ICES Coop. Res. Rep.* *225*, pp. 124–135, Int. Council for the Explor. of the Sea, Copenhagen.
- Lazier, J. R. N. (1995), The salinity decrease in the Labrador Sea over the past thirty years, in *Natural Climate Variability on Decade-to-Century Time Scales*, edited by D. G. Martinson et al., pp. 295–302, Natl. Acad. Press, Washington, D. C.
- Levitus, S., and T. P. Boyer (1994), *World Ocean Atlas 1994*, vol. 4, *Salinity*, NOAA Atlas NESDIS 4, 117 pp., Natl. Oceanic and Atmos. Admin., Silver Spring, Md.
- Levitus, S., R. Burgett, and T. P. Boyer (1994), *World Ocean Atlas 1994*, vol. 3, *Salinity*, NOAA Atlas NESDIS 3, 99 pp., Natl. Oceanic and Atmos. Admin., Silver Spring, Md.
- Manabe, S., and R. J. Stouffer (1988), Two stable equilibria of a coupled ocean-atmosphere model, *J. Clim.*, *1*, 841–866.
- Manabe, S., and R. J. Stouffer (1995), Simulation of abrupt climate change induced by freshwater input to the North Atlantic Ocean, *Nature*, *378*, 165–167.
- Marotzke, J., and J. Willebrand (1991), Multiple equilibria of the global thermohaline circulation, *J. Phys. Oceanogr.*, *21*, 1372–1385.
- McCartney, M. S., and C. Mauritzen (2001), On the origin of the warm inflow to the Nordic seas, *Prog. Oceanogr.*, *51*, 125–214.
- Miyakoda, K., and J. Sirutis (1986), Manual of the E-physics, technical report, 72 pp., Geophys. Fluid Dyn. Lab., Princeton Univ., Princeton, N. J.
- Nilsen, J. E. Ø., Y. Gao, H. Drange, T. Furevik, and M. Bentsen (2003), Simulated North Atlantic–Nordic seas water mass exchanges in an isopycnic coordinate OGCM, *Geophys. Res. Lett.*, *30*(10), 1536, doi:10.1029/2002GL016597.
- Oki, T., and Y. C. Sud (1998), Design of Total Runoff Integrating Pathways (TRIP)—A global river channel network, *Earth Interact.*, *2*(1), 1–37.
- Orvik, K. A., and Ø. Skagseth (2005), Heat flux variations in the eastern Norwegian Atlantic Current toward the Arctic from moored instruments, 1995–2005, *Geophys. Res. Lett.*, *32*, L14610, doi:10.1029/2005GL023487.
- Prinsenber, S. J., and J. Hamilton (2005), Monitoring the volume, freshwater and heat fluxes passing through Lancaster Sound in the Canadian Arctic Archipelago, *Atmos. Ocean*, *43*(1), 1–22.
- Quadfasel, D. A., A. Sy, D. Wells, and A. Tunik (1991), Warming in the Arctic, *Nature*, *350*, 385.
- Quenouille, M. H. (1952), *Associated Measurements*, 241 pp., Butterworths, London.
- Sandø, A. B., and H. Drange (2006), A nested model of the Nordic seas, *Tech. Rep. 268*, Nansen Environ. and Remote Sens. Cent., Bergen, Norway.
- Schauer, U., E. Fahrbach, S. Østerhus, and G. Rohardt (2004), Arctic warming through Fram Strait: Oceanic heat flow from 3 years of current measurements, *J. Geophys. Res.*, *109*, C06026, doi:10.1029/2003JC001823.
- Stommel, H. (1961), Thermohaline convection with two stable regimes of flow, *Tellus*, *13*, 224–230.
- Turrell, W. R., G. Slesser, R. D. Adams, R. Payne, and P. A. Gillibrand (1999), Decadal variability in the composition of Faroe Shetland Channel bottom water, *Deep Sea Res., Part 1*, *46*, 1–25.
- Turrell, W. R., B. Hansen, S. Hughes, and S. Østerhus (2003), Hydrodynamic variability during the decade of the 1990s in the northeast Atlantic and southern Norwegian Sea, *Mar. Sci. Symp.*, *219*, 111–120.
- Woodgate, R. A., and K. Aagaard (2005), Revising the Bering Strait freshwater flux into the Arctic Ocean, *Geophys. Res. Lett.*, *32*, L02602, doi:10.1029/2004GL021747.

S. S. Hjøllø, Bjerknes Centre for Climate Research, Allegaten 70, N-5007 Bergen, Norway. (solfrid.hjollo@gf.uib.no)

C. Mauritzen, Climate Division, Norwegian Meteorological Institute, P.O. Box 43 Blindern, N-0313 Oslo, Norway. (c.mauritzen@met.no)

A. B. Sandø, Nansen Environmental and Remote Sensing Center, Thormøhlensgate 47, N-5006 Bergen, Norway. (anne.britt.sando@nersc.no)